Selective Laser Sintering of Bioactive Glass-Ceramics

J. C. Lorrison*, R. D. Goodridge*, K. W. Dalgarno* and D. J. Wood†

*School of Mechanical Engineering, University of Leeds, Leeds, LS2 9JT, UK
†Leeds Dental Institute, University of Leeds, Leeds, LS2 9JT, UK

Abstract

An initial investigation was held into the feasibility of producing bone replacement implants from a bioactive glass-ceramic using the Selective Laser Sintering (SLS) process. The work presented considers both a direct and an indirect approach, where the material is sintered with a polymer binder and subsequently post-processed. An existing material with potentially suitable biological and mechanical properties was selected from the range of apatite-mullite glass-ceramics in the SiO_2-Al_2O_3-CaO-CaF_2-P_2O_5 series. The viability of using this material with the SLS process was then tested, and the process route and resulting material properties characterised. It is concluded that both direct and indirect SLS processes have potential in the manufacture of personalised bone replacement applications.

Introduction

Implants are commonly constructed from biologically nearly inert materials including metals (stainless steel, titanium alloys), ceramics (alumina, zirconia) and polymers (UHMWPE). A significant draw back of many implants is the difficulty of achieving a secure attachment between the implant and the surrounding bone tissue [1]. Implants are conventionally secured by bone cement or by mechanical means - both of which methods have inherent failings. Bone cement can become loose after a period through cyclic loading and also has the potential for inducing thermal necrosis through an exothermic setting reaction [2]. Mechanical devices, such as pins and screws, are invasive and introduce a potential for stress concentration and infection.

There is therefore a need to produce implants that can be secured by more satisfactory methods. A solution to this problem may be provided by materials that elicit a specific biological response at the bone tissue - material interface, resulting in the formation of a physical bond. Such materials are termed bioactive and often contain an apatitic phase similar to that found in bone tissue, implying superior biocompatibility over other implant materials. They can also be tailored to have similar mechanical properties to human bone [3]. This offers the advantages of a more secure attachment upon implantation than conventional implants and may also reduce the risk of stress shielding and bone degradation that relatively stiff metals can produce.

Current prosthesis techniques generally require a significant degree of skeletal adaptation to suit the chosen device, as skeletal morphology can vary significantly from patient to patient. The economies of scale associated with conventional manufacturing processes lead to a limited range of implants for surgeons to select from and as a result it is often simpler to modify the implant site than the implant itself. A clear drawback of this restriction is the degree of trauma

inflicted upon the implant recipient and the related difficulties encountered in recuperation. It is therefore also desirable to have a process that can produce anatomically shaped prostheses, which could be custom designed and built to suit individual patients.

The ability to produce medical models from CAT scans via rapid prototyping techniques has been established for some time [4]. Such models however have largely been used for surgical procedure planning, being constructed from polymeric materials, allowing surgeons to visualise a patient's physiology prior to any operational procedure. Using the same techniques with bioactive materials may allow custom built implants to be constructed that accurately map to an individual patient's physiology. This would reduce the quantity of bone tissue removed during surgery and potentially increase patient survival rates as well as improve the long-term stability of an implant. The focus of the work presented here has been to investigate the potential of such an approach.

Material Selection

The initial premise, upon which the criterion for material selection was based, focused on the bioactivity of the glass-ceramic. This necessitated the presence of an apatite phase within the material to be chosen and is known to exist in three basic material groups. These are the ceramic hydroxyapatite and the glass-ceramics apatite-wollastonite (A-W) and apatite-mullite (A-M). Of these materials it is known that hydroxyapatite degrades at the high temperatures needed for sintering, while A-W and A-M may have a greater processing potential [5]. In this case the A-M range was selected for initial investigation.

Apatite-mullite glass-ceramics derive their strength from a crystal structure of fine interlocking acicular crystals that are produced after the mechanically inferior base glass is heat-treated [6]. The final choice of material came from a variant within the A-M range, which was thought to have sufficient bioactivity and satisfactory mechanical properties.

Material Production

The base glass produced had the formula described below:

$$4.5SiO_2 \bullet 3Al_2O_3 \bullet 1.6P_2O_5 \bullet 3CaO \bullet 2CaF_2$$
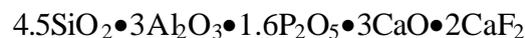
The components were weighed separately on a balance and placed in a container with an agitating bar for mixing in a rotary mill. After an hour the mixture was transferred to a mullite crucible and placed in a furnace at 1450°C for 2 hours, being brought out briefly after 90 minutes and swirled to aid homogenisation. The glass was then shock quenched by pouring directly into water with sufficient speed to prevent crystallisation. Once cooled, the glass was dried before being pulverised with a 250ml puck in a Gy-Ro Rotary Mill for 120 seconds. The powdered glass was then placed in a sieve stack and shaker (Octagon Digital) to separate it into the particle ranges 0-45, 45-90, 90-125 and 125μm and above.

Sinter Station

For both procedures the sinter station used comprised two 125W CO_2 lasers in combination to produce a total power output of 250W and a beam diameter of 1.1mm. As the ceramic materials used do not oxidise, it was not considered necessary to create an inert atmosphere and the experiments were conducted in air at normal atmospheric pressure and room temperature, in a stainless steel chamber lined to prevent material contamination.

Direct Laser Sintering

For the direct laser sintering process, the potential of each range of particle sizes was assessed by attempting to build a single layer, or monolayer. The scan speed was varied from 0-500mm/sec, while the laser power ranged from 0-100W and the degree of scan line overlap was varied across 1/4, 1/2 and 3/4 of the beam width. Of the particle size ranges used, a 1:1 mixture of the 0-45µm and 45-90µm ranges produced the most potentially useful results, spread over a narrow power range of powers (2-4W) and scan speeds (1-3mm/sec) with a half scan line overlap. Table 1 describes the degree of coherence observed for a typical experiment across a range of laser scan speeds. It may be seen that while the processing window for producing coherent monolayers is small, single layer parts can be still be produced at these low powers and scan speeds.

Scan Speed (mm/sec)	Material Appearance
1	Satisfactory coherence
2	
3	Decreasing coherence
….	
3+n	Little or no coherence

Table 1 - Degree of coherence for the 0-45 and 45-90µm particle size ranges

Once the production of single layer scans was established, the construction of multiple layer components was undertaken. The approach used the same parameters as for monolayers, while varying layer thickness. It was found that due to difficulties in spreading the powder, the optimum layer thickness was 0.25mm. Typical monolayer and multiple layer components are shown in Figure 1 where the direction of the scan lines can be clearly seen.
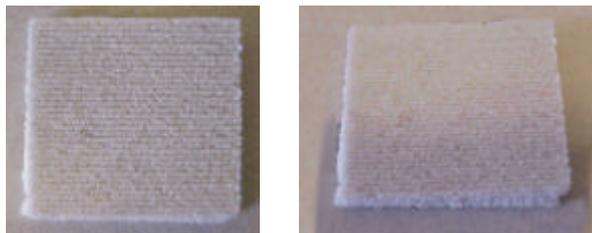
Figure 1 – Single and multiple layer (20×20×2mm) components

Viewing the scan lines with a scanning electron microscope (JSM 35C) indicates that they tend to separate into pairs (Figure 2). This is thought to be due to the first scan line sintering to a partially molten state and then subsequently solidifying. Consequently when the next line is scanned the material in the liquid state, in contact with the previous line, migrates through surface tension towards the solidified material. When the next line is sintered there is therefore less material for it to attach to, creating the gaps while still allowing partial coherence. For this reason the material fractures preferentially along these lines and is relatively brittle.
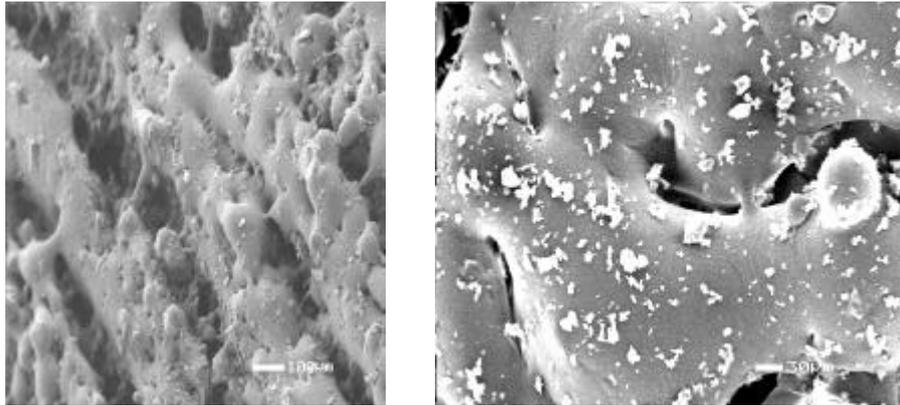
Figure 2 - Micrographs of a sintered monolayer

While the reflective surface prevents visualisation of the interior microstructure of the monolayers it is an indication that a liquid phase is present during the sintering process. Conventional liquid phase sintering occurs when two material phases are present [7]. In this case the material is all of the same composition but over a range of particle sizes. As sintering occurs only at the point where the laser makes contact with the surface of the powder bed, only the smaller particles or those particles on the surface of the powder bed receive a sufficient quantity of thermal energy to cause them to melt. These smaller particles therefore form a liquid phase that is distinct from the larger solid particles and thus it may be said to be liquid phase sintering.

To understand the crystallisation events occurring during the sintering cycle, the processed material was analysed by Differential Thermal Analysis (DTA). A typical trace can be seen in Figure 3 and clearly shows that the peak representing the primary apatite phase has been almost completely removed. This indicates that apatite crystallisation occurs during the sintering process. It may also be seen that the secondary mullite phase remains relatively unchanged. This imposes a need for post-processing to crystallise this phase to gain the improved mechanical and biological properties it imparts. It may also be noted that as crystallisation occurs during the sintering process, the presence of crystalline material in the liquid phase poses a limit to the degree of liquid phase sintering that can occur as it reduces the volume of liquid phase available and hence reduces the overall coherence of the produced components.
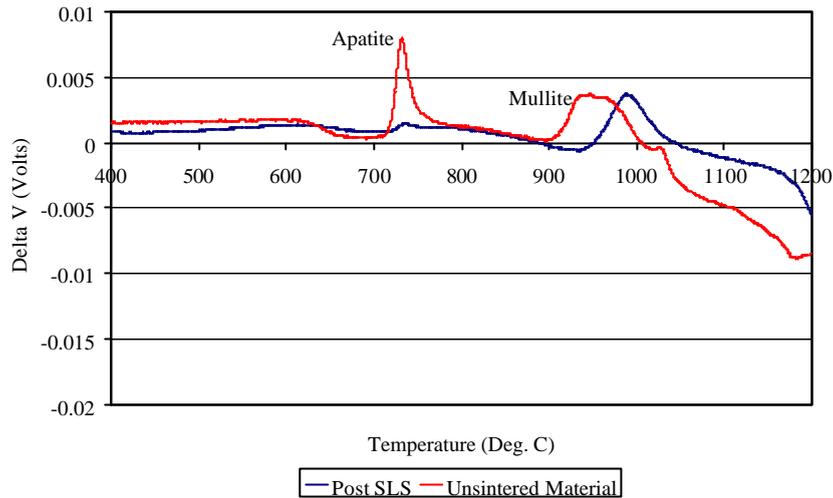
Figure 3 - A DTA trace indicating apatite evolution during laser sintering

Indirect Laser Sintering

The indirect laser sintering approach used an acrylic binder (DTM Corp.) blended at various ratios by mass with the glass-ceramic powder. The scan speed was varied from 0-500mm/sec, while the laser power ranged from 0-150W and the degree of scan line overlap was varied across 1/4, 1/2 and 3/4 of the beam width. It was found that components could be produced over a large range of conditions with scan speeds ranging from 5-500mm/sec and laser powers ranging from 5-150W. No significant difference could be seen between the processing windows of 5%, 10% and 15% binder mixes, although a slight decrease in the powers able to be used was observed for decreasing binder proportions. However, the lower the proportion of binder used, the less fragile the samples appeared and the easier the powder was to handle and spread. Below these proportions a significant decrease in the processing window was observed for a 1% binder mix.

A significant reduction in the processing window was also observed with decreasing particle size, although surface finish and definition were improved. Samples produced from the 0-45μm particle size range were very fragile at all combinations of power and speed. The most promising components were produced from the 45-90μm particle size range, as these had a superior surface finish to larger sized particles, whilst not demonstrating any obvious reduction in the ability to be handled. Typical samples can be seen in Figure 4.

Figure 4 – Indirect components before (left) and after (right) post-processing

5

Multiple layer components were therefore produced from the 45-90μm particle size range with 5% by mass acrylic binder using the process parameters from the components that appeared to have the best coherence. Samples were initially produced at 12W laser power, 150mm/sec scan speed, half scan line overlap and a layer thickness of 0.25mm. Following construction the components are post-processed to produce the final product. During this stage the acrylic binder is burnt off, as this may otherwise render the parts unsuitable for biological use, while inter-particle consolidation occurs concurrently increasing mechanical strength. At the same time the material is also allowed to crystallise fully, evolving the apatite and mullite phases to improve both biological and mechanical properties.

The produced components were post-processed using the following regimes:

A) No post-processing.
B) From room temperature to 1200°C at 10°C/min, dwell for one hour, then cool down.
C) Directly into preheated furnace at 1200°C, dwell for one hour, then cool down.

The success of the post-processing regimes was assessed by measuring the flexural strength and elastic modulus of the samples *via* a three-point bend test giving the results seen in Table 2.

Regime	Flexural Strength (MPa)	Elastic Modulus (MPa)
A	2.43 ± 0.12	459.55 ± 82.54
B	1.51 ± 0.36	1185.76 ± 610.16
C	6.52 ± 0.38	1439.81 ± 197.02

Table 2 - Effect of Post-processing on flexural strength

Prior to post-processing, the samples had a mean flexural strength of 2.43MPa. Following post-processing where the parts were slowly heated using time-temperature profile B, this value was seen to decrease to around 1.51MPa. Higher flexural strengths were achieved when the samples were placed in a furnace pre-heated to 1200°C (as in profile C).

The reasons for this are thought to be due to the fact that the glass-ceramic before SLS is in a non-crystalline, amorphous state and it is only upon heat treatment that crystal phases are evolved. It is thought that the amorphous glassy phase provides the material for liquid phase sintering as the crystal phases have much higher melting temperatures (see Figure 3). If the material is slowly heated there is more time for the development of crystal phases and a corresponding reduction in the quantity of glassy phase material. This would therefore lead to less liquid phase sintering in a slow heat treatment cycle. However, if the material is placed directly into a very hot furnace there may be enough time for liquid phase sintering to occur before crystallisation, hence stronger parts can be produced.

A Joel scanning electron microscope (JSM 35C) was used to study the surface morphology of the post-processed samples, images from which can be seen in Figure 5. Necking at points of contact between adjacent particles can be seen in Figure 5a. The rounding of the

edges of the individual particles seen more clearly in Figure 5b, indicates liquid phase sintering has occurred.
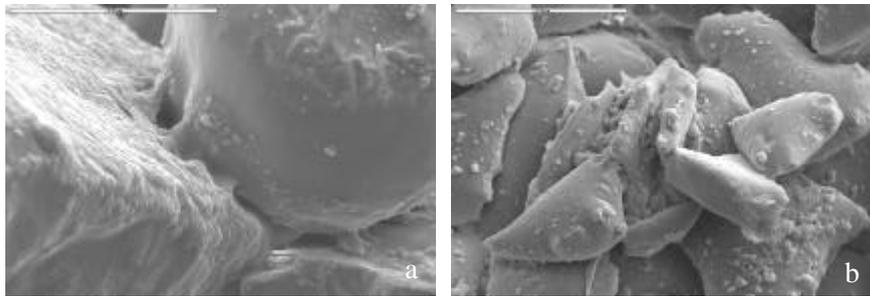
Figure 5 - a and b: Scanning electron micrographs of post-processed LDIG105

Conclusions

The results obtained show that preliminary success has been achieved for producing multiple layer components of sintered material by SLS. For the direct process the best results came when using a 1:1 mixture by mass of the particle size ranges 0-45µm and 45-90µm with a layer thickness of 0.25mm and a half scan line overlap. This approach is however significantly slower than the indirect process, although still capable of producing potentially useable parts (see Table 3).

	Laser Power (W)	Scan Speed (mm/sec)
Direct SLS	2-4	1-3
Indirect SLS	5-150	5-500

Table 3 - Range of successful SLS parameters for direct and indirect methods.

The parts produced to date however exhibit significant signs of brittleness. This arises partially because of the tendency of the scan lines to separate in to pairs, introducing anisotropy. This is further affected by the apatite crystallisation that occurs during the laser sintering process. As the base glass crystallises to apatite the remaining material has less low melting temperature glass available to facilitate liquid phase sintering. This problem may be overcome by either establishing a satisfactory post-processing route, which also evolves the mullite phase, or by using an alternative glass from the same series that would not crystallise during processing, thus leaving enough glass to allow successful liquid phase sintering to occur.

While the processing window for this particular material is quite limited, the processing route has been established and there is scope for trying similar materials, with different thermal properties, while varying particle size arrangements to establish a more flexible system. Further work will address the manufacturing of other glass-ceramic materials and an assessment of the biological and mechanical properties of the parts produced.

The indirect approach has shown that it is possible to fabricate green parts from LDIG105 glass with an acrylic binder and that these can be produced across a much wider range of scanning conditions than has been observed in the direct process. Increasing consolidation of parts with increasing power and decreasing scan speeds was observed, presumably due to an increased amount of energy at the powder surface and thus more liquid phase sintering of the acrylic binder.

A significant reduction in the processing window was observed with decreasing particle size, although the surface finish and definition improved, while the most promising compromise appears to be samples produced from glass with a particle size of 45-90μm.

While the flexural strength test results seen to date indicate the potential for the indirect approach the post-processing regime needs to be modified in order to improve the strength if these parts are to be used in load bearing situations.

References

[1] Vail N, *et al*, Materials for Biomedical Applications, Materials and Design 20 (1999) 123-132.
[2] Lewis G, The fracture toughness of Biomaterials I - Acrylic bone cement, Journal of Materials Education 11 (1989) 429-479.
[3] Hench L and Wilson J, An Introduction to Bioceramics, World Scientific, Singapore (1993) 1-24.
[4] Berry E, *et al*, Preliminary experience with medical applications of rapid prototyping by selective laser sintering, Journal of Medical Engineering and Physics 19 (1997) 90-96.
[5] Ravaglioli A and Krajewski A, Bioceramics, Chapman & Hall, London (1992) 182.
[6] Clifford A and Hill R, Apatite-Mullite Glass-Ceramics, Journal of Non-Crystalline Solids 196 (1996) 346-351.
[7] German R, Sintering Theory and Practice, John Wiley and Sons Inc., New York (1996) 2-8, 68-89 and 226-231.

Acknowledgements